Diffusion Controlled Termination of Linear Polystyrene Radicals in Linear, 4-Arm, and 6-Arm Star Polymer Matrices in Dilute, Semidilute, and Concentrated Solution Conditions

Geoffrey Johnston-Hall and Michael J. Monteiro*

Australian Institute for Bioengineering and Nanotechnology, University of Queensland, Brisbane QLD 4072, Australia

Received October 17, 2007

ABSTRACT: The effect of polymer matrix architecture (polystyrene stars) on the termination of linear polystyrene radical chains was studied in a continually evolving polymer−solvent mixture using the robust and accurate RAFT−CLD−T method. It was found that four distinct regions were observed for the stars analogous to the linear RAFT-mediated polymerizations with chain length dependencies (where $k_t^{i,i} \sim i^{-\alpha}$) for the 4-arm and 6-arm stars in the dilute regime similar to that found for the linear polymer (with α_S and α_L equal to 0.53 and 0.15, respectively). However, the gel onset conversion (x_{gel}) increased with the greater number of arms on the star, in agreement with the Zimm−Stockmayer prediction and in excellent agreement with the theoretical overlap concentration c^*. This supports our previous work that claimed chain overlap is the main cause of the onset of the gel effect in free-radical polymerizations. In concentrated solutions the chain length dependent exponents for linear radicals were much greater in solutions of 4-arm and 6-arm star polymers (with α_{gel} close to $1.82x$ for both) when compared with linear polymer solutions ($\alpha_{gel} = 1.22x$). Because of the increased topological constraints in star polymer solutions, termination was expected to be controlled by reptation (which expects dependencies of 1.5 or 2). However, the dependencies predicted by reptation will only be reached at high conversions (close to the glass transition), suggesting that although solutions of star polymers are more constrained than their linear counterparts, there is still a great deal of matrix mobility on the time scale required for diffusion. The RAFT−CLD−T method also provided a means to determine diffusion coefficients for chain length i using Smoluchowski's equation in the regions where translational diffusion is rate determining.

Introduction

Understanding the diffusion-controlled processes governing radical bimolecular termination in a rapidly evolving polymerization mixture has been extensively debated over the past 60 years especially when auto-acceleration in rate is observed (the "gel effect").[1] There are three concentration regimes available to a polymer−solvent system in a free-radical polymerization (FRP). At low conversions (i.e., low polymer concentrations) the polymer solutions are considered to be "dilute" and polymer coils move independently from one another. Diffusion-controlled termination at these concentrations can be regarded as dependent on solvent−polymer friction, hydrodynamic interactions, and intramolecular segmental mobility. As the polymer concentration is increased beyond the overlap concentration, c^*, polymer−polymer interactions are no longer negligible and influence diffusion. Recently, we showed that the concentration at onset of the gel effect was in excellent agreement with the theoretical concentration for c^*, which is defined as the concentration at which the polymer coils achieve a uniform monomer segment density throughout the reaction mixture.[2] Above this concentration, the solution is regarded as either "semidilute" or "concentrated" (at concentrations much greater than c^*),[3] but unlike the distinct changeover from dilute to semidilute regimes there is no clearly defined concentration that separates the semidilute and concentrated regimes.

It is now well recognized that in the dilute regime, termination is primarily governed by the size of the radical chain length, i. Above c^* and in the semidilute regime, termination is governed by i, the polymer concentration, x, and the size and shape of the surrounding polymer matrix. At even higher polymer concentrations, in concentrated solutions, the effects of polymer concentration and the size and shape of the polymer matrix play an increasingly important role in controlling termination reactions.

Traditionally, due to the broad radical and molecular weight distributions (MWD's) in conventional FRP, it has been extremely difficult to examine the contributions of the polymer concentration and the size and shape of the surrounding matrix on individual terminating chains of identical length.[4] However, Barner-Kowollik et al.[5,6] recently introduced a method based on reversible addition−fragmentation chain transfer (RAFT) polymerization[7,8] to obtain accurate "chain length dependent" (CLD) termination rate coefficients for individual radical chain lengths. The method is based on the linear growth of a narrow distribution of chain lengths with conversion. Thus, at any conversion or time the length of two terminating radicals (i and j) can be assumed to be approximately equal ($i \approx j$). This avoids problems of broad MWD's, and thus short−long termination that plagued analysis of conventional free-radical polymerizations,[4,9−11] and allowed the determination of reliable CLD termination rate coefficients, $k_t^{i,i}(x)$, for a range of radical chain lengths, i, and polymer concentrations, x, from a single experiment.

Recently, we used this technique to study termination during the polymerization of poly(methyl methacrylate) (PMMA).[12] We found that the gel effect corresponded with the theoretical overlap concentration, c^*, and that termination at intermediate and high polymer concentrations did not obey a simple stationary "reptation-like" power law expression,[13,14] but evolved

* Author to whom correspondence should be sent. E-mail: m.monteiro@uq.edu.au.

10.1021/ma702569m CCC: $40.75 © 2008 American Chemical Society
Published on Web 01/16/2008

Scheme 1. RAFT Agents Cumyl Phenyldithioacetate (CPDA), Pentaerythritol Tetrakis(3-(*s*-benzyltrithiocarbonyl)propionate) (4-BTTC), and Dipentaerythritol Hexakis(3-(*s*-benzyltrithiocarbonyl)propionate) (6-BTTC)

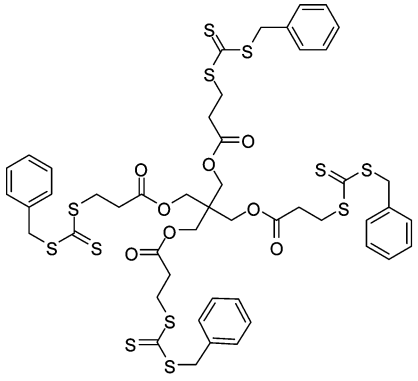

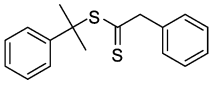

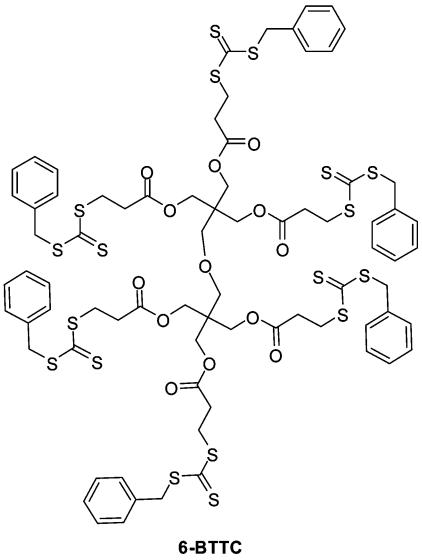

linearly with conversion with $k_t \sim i^{-(1.8x+0.056)}$. The rate coefficient for termination under control by reptation is expected to scale as $k_t \sim i^{-1.5}$ or $k_t \sim i^{-2.0}$.[13−17] Our result brought into question the true influence of the polymer matrix on radical termination.

In 1984, Tirrell[18] postulated that "incisively designed experiments to study matrix and molecular weight effects would hold valuable information for the physical mechanism of macromolecular diffusion in semidilute and concentrated polymer solutions". In particular, star polymers are attractive model systems for studying the effects of hydrodynamic dimensions and topological interactions[19−23] on diffusion-controlled processes. In this work, we have examined the kinetics of termination for linear radicals in dilute, semidilute, and concentrated solutions of star polymers. In particular, we focus on the effect of the polymer coil overlap concentration on the onset of the gel effect, and the effect of macromolecular topology on diffusion-controlled termination in semidilute and concentrated solutions by using the Z-group approach in RAFT-mediated polymerizations.

The Z-group approach[24,25] is ideal for this purpose as linear polymeric radicals propagate and terminate in a polymer star matrix (Scheme 1). Importantly, the Z group approach inherently eliminates any star−star coupling reactions, and the dead polymer consists of only linear dead species. To carry out a RAFT-mediated polymerization via the Z group method, one must use a trithiocarbonate in which the Z group is located at the core molecule (junction point). Growth of the chain arms away from the core means that the trithiocarbonate is always located at the junction point of the star polymer. Therefore, termination between radicals of chain length *i* are surrounded by a star matrix where each arm on the star is also of chain length *i*.

Experimental Section

Chemicals. Styrene (STY, 99%, Aldrich) was purified by filtration through basic alumina (70−230 mesh) to remove inhibitors prior to use. 1,1- azobis (cyclohexanecarbonitrile) (VAZO-88, 99%, DuPont) was purified by recrystallized from methanol twice. All other reagents used in the synthesis of RAFT agents (described below) were obtained from Aldrich (99% purity or greater) and used as received.

Synthesis of Cumyl Phenyldithioacetate (CPDA). Benzyl chloride (40 g) was added dropwise to a mixture of magnesium turnings (7.5 g) in dry diethyl ether (150 mL), and after an initial vigorous reaction, the mixture was refluxed for 3 h to ensure complete reaction. The mixture was then chilled in an ice water bath and carbon disulfide (24.0 g) added dropwise over 30 min. The mixture was then stirred for a further 3 h at 0 °C. The mixture was then poured onto water (300 mL) and the aqueous portion collected following four washes with diethyl ether. A final layer of diethyl ether was added, and the mixture acidified using 30% aqueous HCl. Phenyldithioacetic acid (∼14 g) was collected via rotary evaporation of the ether as a thick orange oil. Following collection, the acid was combined with α-methylstyrene (20% excess, ∼18 g), and a small amount of acid catalyst (0.2 g of paratoluenesulfonic acid) in chloroform (30 mL), and refluxed at 80 °C for 18 h. The crude product was then dissolved in diethyl ether/hexane (1:4) and crystallized at 0 °C to yield orange crystals. These were filtered, washed, and recrystallized a second time using the same procedure described above to yield cumyl phenyldithioacetate as large orange crystals (27.9 g, 30.8%). ^{1}H NMR ($CDCl_3$): $\delta = 1.9$ (s, 6H, $2 \times CH_3$), $\delta = 4.3$ (s, 2H, CH_2), $\delta = 7.2-7.4$ (m, 8H). 7.5 (d, 2H).

Synthesis of Pentaerythritoltetrakis(3-(*s*-benzyltrithiocarbonyl)propionate) (4-BTTC). 4-BTTC was prepared by use of a method analogous to the procedure described for the synthesis of dipentaerythritolhexakis(3-(*s*-benzyltrithiocarbonyl)propionate) described elsewhere.[26]

Triethylamine (20.2 g,) in 50 mL of $CHCl_3$ was added dropwise to a stirred solution of Pentaerythritol (3-mercaptopropionate) (2.44 g, 5 mmol) and carbon disulfide (15.25 g, mmol) in $CHCl_3$ (75 mL) at room temperature. The solution gradually turned deep yellow during the addition. The solution was allowed to stir for an additional 1 h. Benzyl bromide (18.8 g, mmol) dissolved in 50 mL of $CHCl_3$ was added dropwise, and the solution was stirred for a further 2 h. The mixture was poured into a cold solution of 10% aqueous HCl and extracted three times with ethyl acetate to afford a thick yellow oil. The oil was purified by column chromatography using 30% ethyl acetate in *n*-hexane as eluent to obtain the title compound as very thick viscous yellow oil (4.71 g, 82%).^{1}H NMR ($CDCl_3$): $\delta = 2.8$ (t, 8H, CH_2), $\delta = 3.6$ (t, 8H, CH_2), $\delta = 4.2$ (s, 8H, CH_2), $\delta = 4.6$ (t, 8H, CH_2), $\delta = 7.3-7.4$ (20H).

Synthesis of Dipentaerythritolhexakis(3-(*s*-benzyltrithiocarbonyl)propionate) (6-BTTC). 6-BTTC was prepared similarly to the literature procedure.[26] Triethylamine (6.07 g) in chloroform (15 mL) was added dropwise over 30 min to a solution of carbon disulfide (4.57 g) and dipentarythritol hexakis(3-mercaptopropi-

onate) (3.92 g) in chloroform (20 mL) at room temperature. After 1 h, bromobenzene (35 mmol) in chloroform (15 mL) was added dropwise over 30 min. After a further 2 h, the reaction mixture was poured onto an aqueous solution of 10% HCl and extracted 3 times with ethyl acetate to give a yellow oil. The product was purified by using column chromatography and by using a solvent gradient going from hexane/ethyl acetate (3:1) to pure ethyl acetate. The final product was then isolated under vacuum as a think yellow oil (5.62 g, 63%). ^{1}H NMR ($CDCl_3$): $\delta = 2.8$ (t, 12H, CH_2), $\delta = 3.4$ (s, 4H, CH_2), $\delta = 3.6$ (t, 12H, CH_2), $\delta = 4.2$ (s, 12H, CH_2), $\delta = 4.6$ (t, 12H, CH_2), $\delta = 7.3-7.4$ (30H).

A Typical Procedure for the RAFT-Mediated Polymerization of STY. Styrene (2 mL, 8.73 mol/L), VAZO-88 (0.024 g, 49.65 mmol/L), and CPDA (0.057 g, 100 mmol/L) were added to a reaction vessel, degassed by four successive freeze−pump−thaw cycles, sealed under vacuum, and polymerized at 90 °C. Conversion was measured gravimetrically by drying the samples in a vacuum oven at ambient temperature until at constant weight, and the molecular weight distribution was determined by size exclusion chromatography.

A Typical Differential Scanning Calorimetry (DSC) RAFT Polymerization of STY. DSC polymerizations were all performed in duplicate. Styrene (2 mL, 8.73 mol/L), VAZO-88 (0.024 g, 49.65 mmol/L), and CPDA (0.057 g, 100 mmol/L) were added to a reaction vessel, degassed by four successive freeze−pump−thaw cycles, and transferred into gastight DSC pans using a glove bag under nitrogen. The sample weights in the DSC pans ranged between 30 and 65 mg. (The weight in the DSC pans was measured by mass difference between empty and full.) The polymerizations were carried out isothermally at 90 °C, and the heat of polymerization measured by comparing the heat flow from the polymerization pan and an empty pan on a Perkin-Elmer DSC 7 with a TAC 7/DX thermal analysis instrument controller. The DSC instrument was calibrated with a standard indium sample of known mass, melting point temperature, and associated enthalpy change. The rate of polymerization (R_p) and monomer conversions (x) were calculated using literature values for the heat of polymerization of STY ($\Delta H_p = -73$ kJ mol^{-1}).[27]

Size Exclusion Chromatography. Absolute molecular weights of the polymer stars were determined on a size exclusion chromotography (SEC) Shimadzu system with a Wyatt DAWN DSP 5 multiangle laser light scattering (MALLS) detector (683 nm), and a Wyatt OPTILAB EOS interferometric refractometer. THF was used as the eluent with three Phenomenex phenogel columns (500, 104, and 106 Å) connected in series operated at 1 mL/min with column temperature set at 30 °C. The refractive index increments (dn/dc) for the polymers analyzed were determined using the chromatographic method after calibration of the refractometer response with a linear polystyrene standard ($M_w = 110000$, dn/d$c = 0.185$).

Size exclusion chromatography (SEC) measurements of the star and linear polymer were also performed using a Waters Alliance 2690 Separations Module equipped with an autosampler, column heater, differential refractive index detector, and a photodiode array (PDA) connected in series. HPLC grade tetrahydrofuran was used as eluent at a flow rate of 1 mL min^{-1}. The columns consisted of three 7.8 × 300 mm Waters Styragel GPC columns connected in series, comprising two linear UltraStyragel and one Styragel HR3 columns. Polystyrene standards ranging from 2000000 to 517 g mol^{-1} were used for calibration.

Calculations

Determination of Conversion and Chain Length Dependent Termination Rate Coefficients. Conversion and chain length dependent termination rate coefficients, $k_t^{i,i}(x)$, were determined using the RAFT−CLD−T method described elsewhere.[4−6,12] Due to the moderate reaction temperature (90 °C) self-initiation of styrene through thermal reactions cannot be excluded. An expression for the rate of auto-initiation,[28] R_{th}, was included in the calculation of the time dependent termination rate coefficient, $k_t(t)$

$$k_t(t) = \frac{2fk_d[I]_0e^{-k_dt} + R_{th} - \dfrac{d\left(\dfrac{R_p(t)}{k_p\left([M]_0 - \int_0^t R_p(t)\,dt\right)}\right)}{dt}}{2\left(\dfrac{R_p(t)}{k_p\left([M]_0 - \int_0^t R_p(t)\,dt\right)}\right)^2} \quad (1)$$

where $[I]_0$ is the initial initiator concentration, $[M]_0$ is the initial monomer concentration, $[M]_x$ is the instantaneous monomer concentration (at time x), k_d is the initiator decomposition rate coefficient, k_p is the propagation rate coefficient, and f is the initiator efficiency. The auto-initiation rate constant, R_{th}, was determined experimentally by carrying out polymerizations in the absence of VAZO-88 and measuring R_p at low conversions (<5%). From this data and a constant k_t (1×10^9 L mol^{-1} s^{-1}) in eq 1, R_{th} was determined (see Table 1). This value was used as constant over the full conversion range. It should be noted that, under the experimental conditions in this work, $k_t(t)$ remained unchanged even when R_{th} was not included in eq 1.

From $k_t(t)$ found using eq 1, the chain length and conversion dependent termination rate coefficient, $k_t^{i,i}(x)$, was determined by factoring in the conversion dependent chain length during a RAFT-mediated polymerization. The theoretical evolution of chain length, i, with conversion, x, was used as the experimental M_n was close to theory

$$i = \frac{[M]_o x}{([RAFT]_0 - [RAFT]_x) + af([I]_0 - [I]_x) + a\left(\int_0^{t_x} R_{th}\,dt\right)} \quad (2)$$

where $[RAFT]_0$ is the initial RAFT agent concentration, $[RAFT]_x$ is RAFT agent concentration at x, a is the mode of termination (a equals 1 for termination by combination and 2 for disproportionation), $[I]_0$ is the initial initiator concentration, and $[I]_x$ is the instantaneous initiator concentration. Rate coefficients used in eqs 1 and 2 were taken from reliable literature sources and are listed in Table 1.

Table 1. Kinetic Parameters Used for Analysis of $k_t^{i,i}$ from the RAFT-mediated Bulk Polymerization of Styrene (STY) Initiated with 1,1-Azobis(cyclohexanecarbonitrile) (VAZO-88) at 90 °C, in the Presence of Cumyl Phenyldithioacetate (CPDA), Pentaerythritoltetrakis(3-(*s*-benzyltrithiocarbonyl)propionate) (4-BTTC), and Dipentaerythritol Hexakis(3-(*s*-benzyltrithiocarbonyl)propionate) (6-BTTC)

	T (°C)	k_p (L mol^{-1} s^{-1})	k_d (s^{-1})	R_{th} (mol L^{-1} s^{-1})[a]	f	ΔH_p (kJ mol^{-1})
STY	90	900[73]	2.7×10^{-5} [74]	2×10^{-9}*	0.70	−73.0[27]

[a] Determined in the current study.

Accuracy of the RAFT−CLD−T Method To Determine $k_t^{i,i}$. A reviewer questioned the accuracy of the RAFT−CLD−T method when using RAFT agents with low chain transfer constants. Therefore, in this section, we discuss the robust nature of the RAFT−CLD−T method and the criteria required to obtain accurate k_t values for chain length dependence. Generally, the RAFT−CLD−T method has been found to be robust and able to determine accurate values of $k_t^{i,i}(x)$ for a range of monomers and under a range of experimental conditions, both as a function of increasing chain length[6,29−31] and increasing conversion.[4,12,32−34] However, the method is only accurate if the rate of polymerization is unaffected, and RAFT agents that

Scheme 2. Illustration of the Z-Group Approach Used in the Preparation of Star Polymers via RAFT, Where Bimolecular Termination in This Approach Occurs between Linear Radicals in a Matrix of Star Polymers

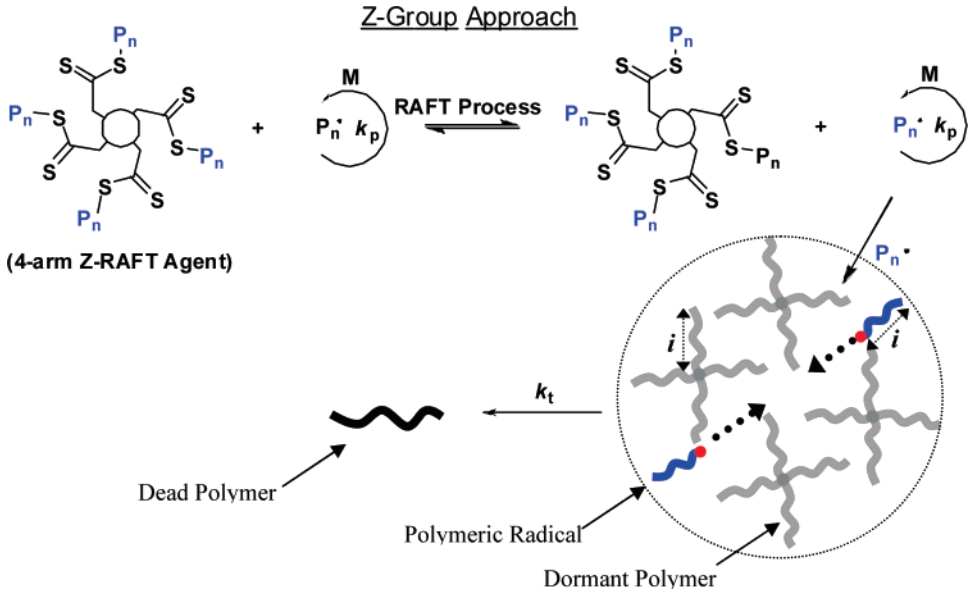

undergo either slow fragmentation[35] (SF) or intermediate radical termination[36] (IRT) are absent.[30,37] Hence, the RAFT agent cumyl dithiobenzoate (CDB) cannot be used to obtain $k_t^{i,i}$ for styrene polymerizations.[36] Importantly, termination should be dominated by chain lengths close to *i*, however, should there be substantial "short−long" termination (such as in conventional FRP) the method is no longer valid.[4] We have previously published detailed simulations on the validity of the RAFT−CLD−T method.[4]

It has been postulated that RAFT agents with poor leaving (R) groups (Scheme 2) may also compromise the accuracy of the RAFT−CLD−T method. Feldermann et al.[31] considered the effects of the R group on the accuracy of determining $k_t^{i,i}$ using the RAFT−CLD−T method and eq 3 to convert average k_t *vs* *x* profiles to $k_t^{i,i}$ *vs* *i*.

$$i = \frac{[M]_o x}{[RAFT]_0} \tag{3}$$

Figure 1A shows their results[31] for the effect of increasingly poor leaving groups (benzyl, α-methylbenzyl and cumyl) on the log $k_t^{i,i}$ vs log *i* profiles for the RAFT-mediated polymerizations of styrene at 80 °C. It is found that as the leaving group

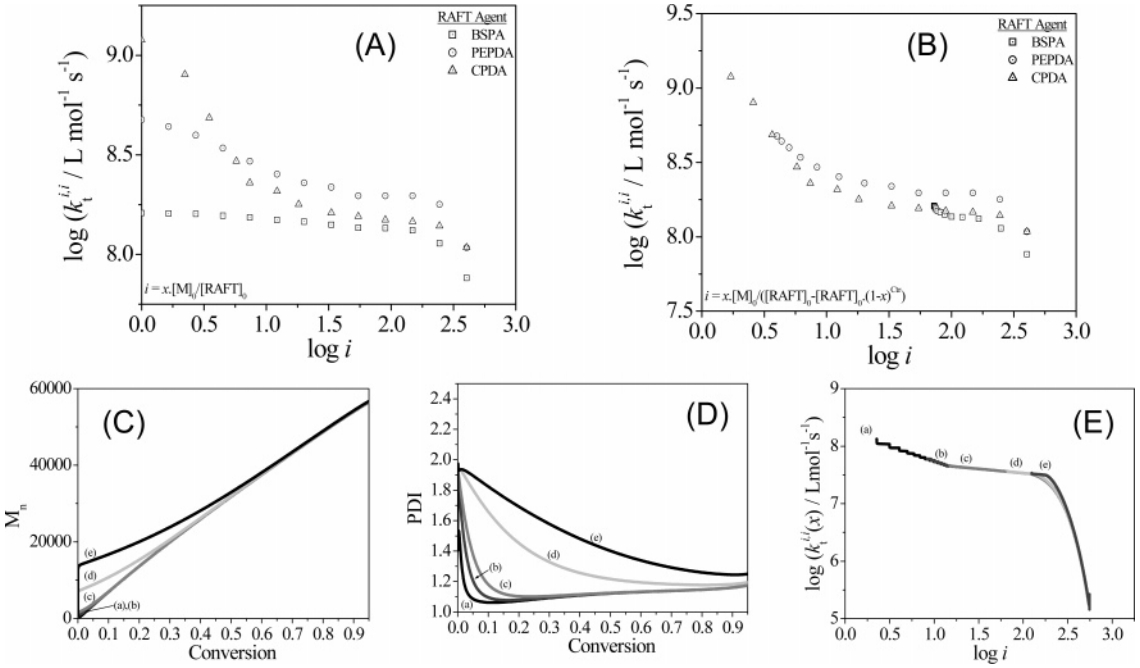

Figure 1. (A) Reproduced data from Feldermann et al.[31] where they used eq 3 to convert *x* to *i*, for the RAFT-mediated polymerization of STY at 80 °C using 3-benzylsulfanylthiocarbonylsulfanylpropionic acid (BSPA, 11.0 mM), phenylethyl phenyldithioacetate (PEPDA, 11.0 mM), and cumyl phenyldithioacetate (CPDA, 11.0 mM), with 2,2-azobis(isobutyronitrile) (AIBN, 17 mM) as initiator (B) the same data reanalyzed using the more accurate eq 2. Kinetic simulations varying the pre-equilibrium chain transfer constant ($C_{tr(Pre)}$) to RAFT and maintaining a high $C_{tr(Main)}$ = 1000 for styrene (STY, 8.73 M) at 90 °C using 1,1- azobis (cyclohexanecarbonitrile) (VAZO-88), (C) number-average molecular weight (M_n) vs conversion, (D) polydispersity (PDI) vs conversion, and (E) log $k_t^{i,i}(x)$ vs log *i* profiles. (a) $C_{tr(Pre)}$ = 1000, (b) $C_{tr(Pre)}$ = 500, (c) $C_{tr(Pre)}$ = 100, (d) $C_{tr(Pre)}$ = 10, and (e) $C_{tr(Pre)}$ = 5. The concentration of RAFT agent and initiator used were $[RAFT]_0$ = 12.5 mM and $[I]_0$ = 6.75 mM.

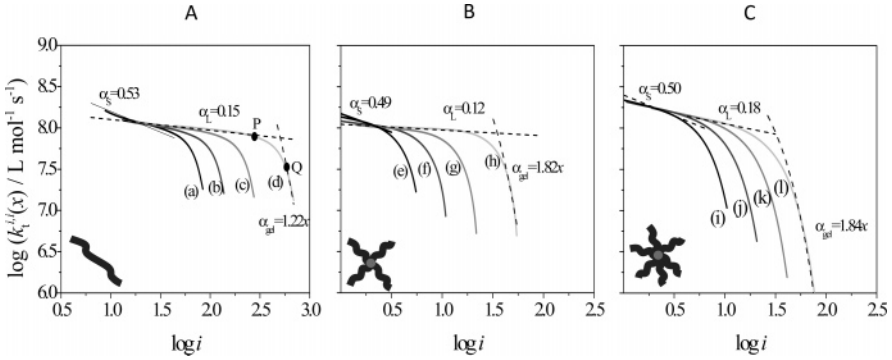

Figure 2. Effect of chain length and conversion on the termination rate coefficient, $k_t^{i,i}(x)$, vs radical chain length, *i*, for the reversible addition−fragmentation chain transfer (RAFT) mediated polymerization of styrene (STY, 8.73 M) at 90 °C using 1,1- azobis (cyclohexanecarbonitrile) (VAZO-88) as initiator (A) linear RAFT agent, (B) 4-arm star RAFT agent, and (C) 6-arm-star RAFT agent. In part A, the concentrations of RAFT agent used are approximately (a) 100 mM, (b) 50 mM, (c) 25 mM, and (d) 10 mM, in part B, the concentrations of RAFT agent used are approximately (e) 100 mM, (f) 50 mM, (g) 25 mM, and (h) 10 mM, and in part C, the concentrations of RAFT agent used are approximately (i) 200 mM, (j) 100 mM, (k) 50 mM, and (l) 25 mM.

becomes poorer there is increasing deviation in the $k_t^{i,i}$ profiles (i.e., lower k_t values at the same *i*) for small values of log *i* when compared with the ideal case (i.e., CPDA in this example). It should be recognized that for a RAFT agent with a poor leaving group, the M_n values at very low conversions are much higher than predicted for a RAFT agent with a good leaving group (see Figure 2 in ref 31), making the use of eq 3 inaccurate. We have therefore recalculated their data (see Figure 1 in ref 31) using our more accurate eq 2[38,39] (Figure 1B), and find that regardless of the RAFT agent used, all the k_t profiles are very similar regardless of *i*. This supports our earlier work[4] demonstrating that the RAFT−CLD−T method is even more robust and accurate across a wide range of experimental conditions than Barner-Kowollik and coworkers anticipated, and should be considered as revolutionary as the pulsed laser polymerization (PLP) method[40] used to obtain accurate values for k_p.

To further support the RAFT−CLD−T method, we carried out simulations by varying the chain transfer coefficient for the RAFT pre-equilibrium ($C_{tr(Pre)}$) step from 1000 (a very good leaving group) down to 5 (a very poor leaving group), while maintaining a high C_{tr} for the main equilibrium steps. The simulations are under similar starting concentrations of RAFT agent, monomer and initiator as that used in this work. Accurate rate parameters found from the literature (Table 1), and a composite k_t model[4,12,34] determined from the data for CPDA (Scheme 1) in this work (since a cumyl moiety is a good leaving group[31]) were used in the simulations. Figure 1C shows that with a decrease in $C_{tr(Pre)}$, the M_n increased to high initial values and then grew relatively linearly with conversion, converging with the M_n profile for $C_{tr(Pre)}$ equals 1000 at high conversions (approximately 50% for $C_{tr(Pre)}$ equals 5). The polydispersity index (PDI) values also show the same trend, with lower $C_{tr(Pre)}$ values resulting in higher initial PDI's. The log $k_t^{i,i}(x)$ vs log *i* profiles for each of the $C_{tr(Pre)}$ values are given in Figure 1E, and show that using true *i* values (i.e., eq 2), all the measured k_t profiles are identical and in agreement with the experimental data in Figure 1B. These results provide strong support for the claim that the RAFT−CLD−T method is accurate even when using a RAFT agent with a poor leaving group.

Thus, the RAFT−CLD−T method has also been used to obtain accurate k_t data as a function of *i* with *x* for methyl methacrylate (MMA) with cyanoisoprop-2-yl dithiobenzoate,[6,12] and vinyl acetate (VAc) with 2-ethoxythiocarbonylsulfanyl-propionic acid methyl ester,[33] despite the observation of poor leaving group effects in these reactions. In this current work, RAFT agents were used with two different leaving groups: cumyl and benzyl. Rate retardation or inhibition was not observed, indicating SF and IRT were absent. In addition, we found (see Supporting Information) that the M_n's for the linear, 4-arm, and 6-arm stars were all close to "ideal" behavior, even at the beginning of the polymerizations (i.e., low conversions), indicating that poor leaving group effects were not present under our experimental conditions. We only take data above 5% conversion for all polymerizations to obtain the k_t profiles.

Determination of Theoretical *c for Star Polymers.** Rather than being a single defined concentration, *c** occurs across a concentration range as the dimensions of polymer coils change with concentration in the vicinity of *c**. To account for this, it has been suggested that *c** can be defined as[41]

$$\frac{3}{4\pi}\frac{M_n}{R_g^3 N_A} < c^* < \frac{M_n}{R_g^3 N_A} \tag{4}$$

where the radius of gyration, R_g, can be calculated (for linear polymer) via the expression:[42]

$$R_g = \sqrt{\frac{C^\infty M_n l^2}{mw}} \tag{5}$$

where mw is the monomer molecular weight, *l* the length between two monomer units, C^∞ the expansion factor, and N_A Avogadro's constant.

For large flexible Gaussian polymers, Zimm and Stockmayer[42−44] predicted a quantitative relationship between the R_g for a star polymer of *f* arms and a linear polymer with equal molecular weight according to the following equation:

$$g = \frac{R_{g(s)}^2}{R_{g(l)}^2} = \frac{3f-2}{f^2} \tag{6}$$

Equation 6 predicts that the mean-square radius of gyration of a star polymer, $R_{g(s)}^2$, will be smaller compared with the mean-square radius of gyration of a linear polymer, $R_{g(l)}^2$, by a factor of *g*, which is approximately 0.625 for a polymer with 4 arms and 0.444 for a polymer with 6 arms. It follows from eq 4 and eq 6 that the theoretical *c** for star polymers should increase according to

$$\frac{c^*_{(linear)}}{c^*_{(star)}} = \left(\frac{3f-2}{f^2}\right)^{\frac{3}{2}} \tag{7}$$

Results and Discussion

The three RAFT agents used in this work (Scheme 2) gave linear (CPDA), 4-arm star (4-BTTC), and 6-arm star (6-BTTC) dormant polystyrene species. The polymerizations were carried out in bulk at 90 °C over a range of RAFT and VAZO-88 concentrations (see Table S1 in the Supporting Information section). The evolution of conversion with time, M_n and PDI with conversion, and representative SEC molecular weight distributions are also given in the Supporting Information, and theoretical predictions for M_n agreed with data found from experiment. MWDs for the 4- and 6-arm star polymers are typically broader than for linear polymer, due to the formation of some low molecular weight dead polymer.[24,25] The 3-dimensional $k_t^{i,i}(x)$ plot over i and x for the three sets of data are also given in the Supporting Information section, and from this data the influence of polymer chain length on termination can be observed for the three sets of RAFT-mediated polymerizations (Figure 2).

Figure 2 shows the $k_t^{i,i}(x)$ profiles over the conversion range at different RAFT concentrations for linear, 4-arm, and 6-arm stars. The 4-arm and 6-arm star RAFT agent's, 4-BTTC and 6-BTTC, are Z-group RAFT agents. Unlike linear RAFT agents the chain length of terminating radicals, i, are smaller than the chain length of surrounding (star−matrix) polymer, N, by a factor equal to the number of star arms, f (see Scheme 1, $i = N/f$). In these systems, the propagating radical chain length i grows at the same rate as N, and therefore, it allows one to compare termination between two i radicals in a linear or star matrix depending on the RAFT agent used. In Figure 2, the power law dependence α (where $k_t^{i,i}(x) \sim i^{-\alpha}$) is given for the three matrices in the dilute regime (where α_s is the short chain region and α_L is the long chain region), and in the concentrated regime (defined as α_{gel}).

We define the semidilute regime as the region starting from the gel onset point (point P in Figure 2A) until the concentrated regime (point Q). In this region, topological constraints of the surrounding matrix begin to impede radical mobility and termination slows considerably. It is obvious that trying to quantify the semidilute region is difficult, therefore, we have focused our discussion in this article on (1) the dilute regime, (2) the onset of the semidilute regime (i.e., the gel onset, point P), and (3) the concentrated regime (following point Q) (vide infra).

Termination in the Dilute Regime. In recent years, opinion on termination in dilute solutions has shifted from the classical belief that chain end mobility is rate determining[45] in favor of what has been termed "composite" behavior.[6,46,47] For the linear polymer (Figure 2A), it is clear that two distinct processes dominate termination in dilute solutions. At very short chain lengths $k_t^{i,i}$ is controlled by center-of-mass diffusion, and scales according to the radical chain length, i, with a power law exponent of $\alpha_{S(linear)} \sim 0.53$, in agreement with predictions of the Stokes−Einstein equation.[3] At a crossover chain length of $i_{SL(linear)} \sim 18$, chain-end segment mobility becomes rate determining and $k_t^{i,i}$ scales with a "long" chain exponent $\alpha_{L(linear)} \sim 0.15$, in agreement with theoretical predictions for segmental diffusion.[48−50]

For the star polymer solutions, this composite behavior becomes less well-defined with increasing star arms. The reason for this arises from the radical chain lengths being much smaller by a factor of f to the polymer matrix, which in some cases led to the onset of the gel effect prior to the crossover from "short" to the "long" chain regime. However, α_s and α_L were determined with a best fit for the 4-arm and 6-arm stars and gave comparable values to the linear system, suggesting that the matrix architecture had little influence on termination in the dilute regime.

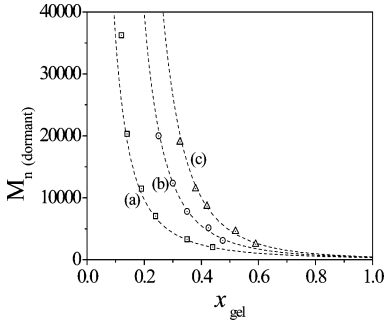

Figure 3. M_n vs conversion profiles determined at onset of the gel effect (x_{gel}) from the bulk reversible addition−fragmentation chain transfer (RAFT) mediated polymerization of styrene at 90 °C using (a) linear (□), (b) 4-arm star (○), and (c) 6-arm star (△) RAFT agents. Data points were determined directly from experimental log $k_t^{i,i}$ vs log N data, *and* 3-dimensional surface analysis data (see Supporting Information).

Gel Effect Onset (Start of the Semidilute Regime). We wanted to gain insight into the effect of star topology on the gel onset point and, in particular, examine the effects of hydrodynamic dimensions and physical cross-links on termination. Because of the higher segment densities in star polymers, it may be expected that c^* will be affected by the number of star polymer arms and that the central tethered points may greatly restrict the intermolecular mobility of radical and matrix chains. Figure 3 shows the effect of M_n on the gel onset conversion, x_{gel}, for linear, 4-arm, and 6-arm stars. As the polymer architecture was changed from linear through to 6-arm star at any value for M_n of the dormant polymer, the x_{gel} increased, suggesting that the hydrodynamic volumes of the dormant polymer plays an important role. The smaller the hydrodynamic volume the greater x_{gel}, usually found with increasing arms on a star polymer.

Because of often conflicting evidence and opinion, the cause of the gel effect has been the subject of some debate (see ref 51). Much of this uncertainty can be attributed to the use of polymer matrices and polymeric radicals with a wide range of chain lengths,[4] a problem that is overcome by using "living" radical polymerization in which a narrow chain length distribution is generated. In our previous work, we found excellent agreement between x_{gel} and the theoretical overlap concentration, c^*, for a variety of monomers including methyl acrylate, methyl methacrylate and vinyl actetate.[12] Compared with the linear polymer, star polymers are governed by higher polymer-segment densities and possess smaller solution dimensions than their linear counterparts (at equivalent M_n);[43,52,53] therefore, c^* increased as a function of increasing arms, f. Figure 4 compares the theoretical profiles for c^*_{min} and c^*_{max} using eq 4 with experimental values from Figure 3. The experimental x_{gel} values were found within the theoretical range for c^* for linear, 4-arm, and 6-arm stars, supporting our previous results that c^* is the major cause of the gel onset under isothermal conditions. It should also be noted that the molecular weights and polymer concentrations are well below predictions based on chain entanglements.[13,5455]

The power law dependencies, α, of x_{gel} with M_n (i.e., $x_{gel} \sim M_n^{-\alpha}$) decrease from 0.45, 0.35 to 0.3 for linear, 4-arm, and 6-arm stars, respectively. Turner et al.[56−59] identified that the gel onset in an unentangled polymer matrix would have a dependence of 0.5 (for chain overlap) that increased to 1 in an entangled matrix. Our α data for the linear polymer is close to

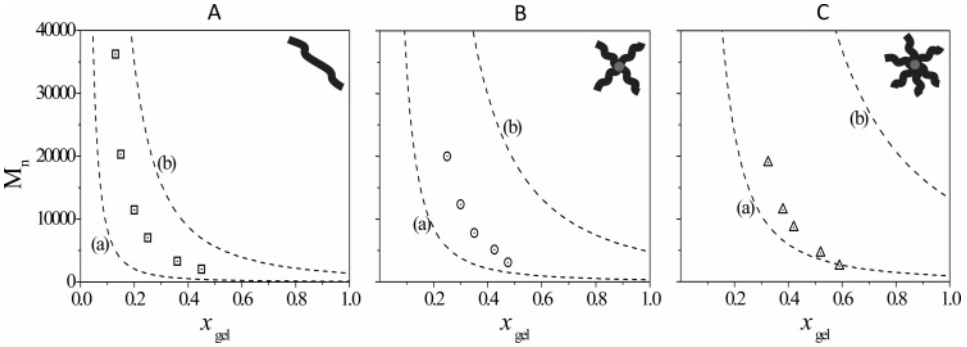

Figure 4. M_n vs conversion determined at onset of the gel effect (x_{gel}) from the bulk reversible addition−fragmentation chain transfer (RAFT) mediated polymerization of styrene at 90 °C using (A) linear (□), (B) 4-arm star (○), and (C) 6-arm star (△) RAFT agents. The theoretical limits for the overlap concentration, c^*, curve (a) $c^* > (3M_n)/(4\pi R_g^3 N_A)$, and (b) $c^* < M_n/(R_g^3 N_A)$. Data points were determined directly from experimental log k_t vs log N data, *and* 3-dimensional surface analysis data (see Supporting Information). Values for the c^* region were calculated using eq 5 and mw = 104.15 g mol^{-1}, $l = 2 \times 1.54$ Å,[75] and $C^\infty = 9.89$.[75]

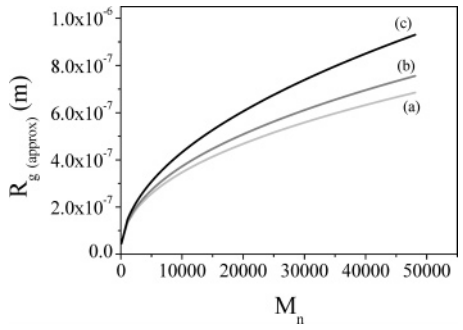

Figure 5. Plot of the approximate radius of gyration, R_g, vs M_n, for (a) linear, (b) 4-arm star, and (c) 6-arm star polymer at onset of the gel effect, during the bulk reversible addition−fragmentation chain transfer (RAFT) mediated polymerization of styrene at 90 °C. Data was determined from the plot of the gel effect onset, x_{gel}, and M_n (see Figure 2) by assuming $c^* = M_n/(R_g^3 N_{av})$.

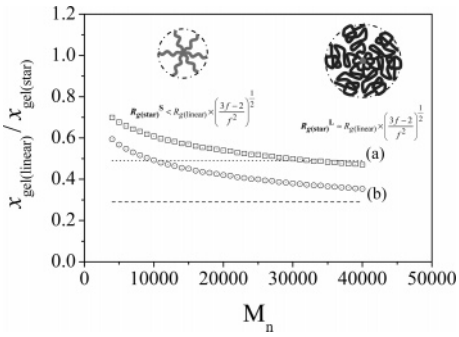

Figure 6. The ratio for the conversion at onset of the gel effect (x_{gel}) for linear to star polymer ($x_{gel(linear)}/x_{gel(star)}$) determined for the polymerization of (a) 4-arm star (□), and (b) 6-arm star (○) polystyrene (PSTY) at 90 °C is plotted against molecular weight (M_n). $x_{gel(linear)}/x_{gel(star)}$ profiles approach the theoretical Zimm−Stockmayer expression[43] (ie c^*_{star}/c^*_{linear}) for 4-arm star polymer (dotted line), and 6-arm star polymer (dashed line), at high M_n. Low M_n stars deviate from theory due to steric effects close to the core leading to $x_{gel(star)} \sim x_{gel(linear)}$ at low M_n (refer to inset illustration).

theory for an unentangled matrix, but surprisingly a decrease in α with an increasing number of arms on the star is observed. In fact, it would be expected that if entanglements do cause the onset of the gel, α would increase toward 1 from linear to 6-arm star polymer as the tethered points in the star could act as entanglement points. The major conclusion from these results implies that chain overlap and not entanglements are the cause of the gel effect.

On the basis of the excellent correlation between c^* and x_{gel}, the radius of gyration at x_{gel} can be calculated from the upper limit in eq 4 (Figure 5). It can be seen that R_g is lower for the 4-arm and 6-arm stars compared with the linear polymer, as expected, with the 6-arm star appearing to be the smallest. This suggests that the greater the arms on the star the more compact the structure; in agreement with literature.[43,52,53]

Since c^* is equivalent to x_{gel}, it is expected based on the Zimm−Stockmayer expression that the following equation be satisfied:

$$\frac{x_{gel(linear)}}{x_{gel(star)}} = \left(\frac{3f-2}{f^2}\right)^{\frac{3}{2}} \qquad (8)$$

Figure 6 shows that eq 8 is satisfied only at high M_n values in which the experimental data converges toward the Zimm−Stockmayer relationship (dashed lines). For the high molecular weight 4-arm star polymer, a value of approximately 0.49 is approached at the high molecular weight limit of ∼40000. Similarly, the six arm star polymer shows good agreement with theory in the high molecular weight region; approaching a value of ∼0.34. At low molecular weights the $x_{gel(linear)}/x_{gel(star)}$ ratios were well above the predictions from eq 8, approaching a value in the vicinity of ∼1. This is not unexpected since the Zimm−Stockmayer expression was developed for swollen Gaussian chains. In the case of short-arm star polymers the high polymer segment densities cause congestion leading to stiffening of the star arms close to the core[22,53,60−62] (see inset illustration in Figure 6). Hence, the deviation to higher ratios at lower molecular weight stars.

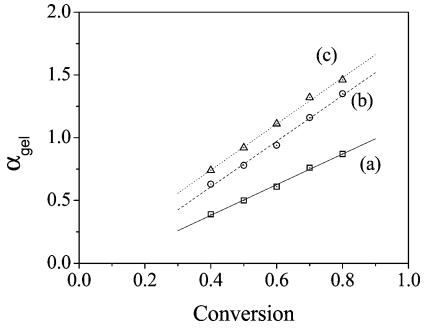

Figure 7. Chain length dependent exponent, α_{gel}, profiles determined in the gel regime (i.e., between 50 and 70% conversion, for the power law expression $k_t \propto i^{-\alpha gel}$) are given as a function of the weight fraction of polymer, x, determined for the bulk polymerization of styrene (STY, 8.73 M) at 90 °C using 1,1- azobis (cyclohexanecarbonitrile) (VAZO-88) as initiator and a (a) linear RAFT agent (□), (b) 4-arm-star RAFT agent (○), and (c) 6-arm-star RAFT agent (Δ). Linear regression led to the following best fit expressions for each data set: (a) $1.22x - 0.11$, (b) $1.82x - 0.10$, and (c) $1.84x + 0.01$.

Table 2. Comparison of Chain Length Dependent Exponents in the Power Law Expression $k_t \propto i^{-\alpha}$ Determined for the Short Chain Dilute Regime, α_S, the Long Chain Dilute Regime, α_L, and Gel Regime, α_{gel}, in the Polymerization of Styrene (STY) at 90 °C[a]

	(T) °C)	α_S (±6%)	α_L (±5%)	α_{gel} (±5%)
STY-L/L	90	0.53	0.15	$1.22x - 0.11$
STY-L/4-S	90	0.49	0.12	$1.82x - 0.10$
STY-L/6-S	90	0.50	0.18	$1.84x + 0.01$

[a] Results are given for the termination of linear radicals in a linear matrix, L/L, and linear radicals in a 4-arm star matrix, L/4-S, and 6 arm star matrix, L/6-S. x = weight fraction of polymer

Scheme 3. General Mechanism for Diffusion Controlled Termination, Which Can Be Described by a Three-Step Process Involving (1) Translational Diffusion, (2) Segmental Diffusion (i.e., Rearrangement), and (3) Radical−Radical Reaction

$$P_i^{\bullet} + P_i^{\bullet} \underset{k_{-trans}^{i,i}}{\overset{k_{trans}^{i,i}}{\rightleftharpoons}} P_i^{\bullet}\text{---}P_i^{\bullet}$$

$$P_i^{\bullet}\text{---}P_i^{\bullet} \underset{k_{-segm}^{i,i}}{\overset{k_{segm}^{i,i}}{\rightleftharpoons}} P_i^{\bullet}/P_i^{\bullet}$$

$$P_i^{\bullet}/P_i^{\bullet} \xrightarrow{k_{chem}^{i,i}} Dead_{i+i}$$

Above c^*, it is difficult to quantify the semidilute regime as $\log k_t^{i,i}(x)$ decreases nonlinearly with $\log i$ up to the concentrated regime, regardless of the matrix architecture. However, it was qualitatively observed that at the same RAFT agent concentrations for the linear, 4-arm, and 6-arm stars, the width of semidilute regime became smaller (see Figure 2). This supports our earlier postulate that having tethered points above c^* results in a more constrained polymer matrix, resulting in slower diffusion of polymeric radicals. This should be more visible in the concentrated regime.

Termination in the Concentrated Regime. It can be seen from Figure 2 that the concentrated regime occurs well beyond the onset of the gel effect. In this region, $k_t^{i,i}$ becomes significantly dependent upon the polymer concentration and chain length. The effect of polymer architecture can be analyzed by comparing α_{gel} exponents. Figure 7 shows a linear increase in α_{gel} with conversion for the three polymer systems (data given in Table 2). This conversion dependent increase is in agreement with our previous findings[12] as well as observed self-diffusion measurements.[63,64] The 4-arm and 6-arm star matrices gave similar α_{gel} functions (both close to $\sim 1.82x$), and were much greater than for the linear matrix ($\sim 1.22x$). This supports the postulate that the restriction placed upon the matrix by tethering the arms together produce more obstacles for the linear polymeric radicals to diffuse past. At first sight this could be explained by reptation,[13,14] which would predict that α_{gel} is stationary and close to 1.5 or 2. However, our data show that α_{gel} is dependent upon conversion and will only reach values close to 1.5 at conversions around 80%, in the vicinity of the start of the glass regime. This suggests that although there are constriction points in the polymer matrix there is still a great deal of matrix mobility on the time scale required for diffusion, and that the linear radicals are not confined to a tubelike surrounding; as prescribed by reptation.

Diffusion Coefficients of *i* Radicals in Linear, 4-Arm, and 6-Arm Star Polymer Matrices. It has been common practice to use indirect methods (such as pulsed field gradient (PFG) NMR[17,63,65,66]) to study the effects of polymer concentration and polymer matrix on termination of individual radicals. These methods measure how translational diffusion of individual chains are affected by chain size, matrix size, and total polymer concentration. Values of $k_t^{i,i}(x)$ are then calculated with these diffusion coefficients using Smoluchowski equation[67] (eq 9) and including a capture radius "r", and probability factor "p", to yield

$$k_t^{i,j} = 2\pi N_{av} p(D_i + D_j) r \tag{9}$$

The termination constant derived from eq 9 is based solely on translational diffusion, and cannot be used to obtain rate constants where termination is controlled by segmental diffusion particularly for long chains in dilute solutions. Benson and North[48,68] were the first to describe termination in terms of a three step process involving translational diffusion, segmental diffusion, and radical−radical annihilation (Scheme 3). For the case that translational diffusion is slow (and therefore rate controlling), the termination rate coefficient is directly proportional to the rate coefficient for association by translational diffusion, k_{trans}; since (by definition) any two polymeric radicals that encounter one another will terminate,[69] therefore eq 9 gives valid termination rate constants.

$$k_t^{i,i} = k_{trans}^{i,i} \tag{10}$$

However, when the coefficient for segmental diffusion, k_{segm}, is rate determining, termination is a function of k_{segm}, k_{trans}, and

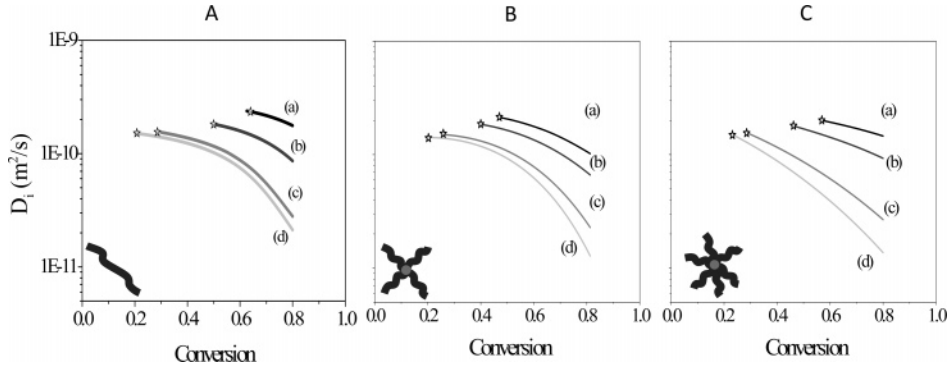

Figure 8. Plot of the diffusion constant, D_i, vs conversion calculated from termination rate coefficient data (using the Smoluchowski equation) for the reversible addition−fragmentation chain transfer (RAFT) mediated polymerization of styrene (STY, 8.73 M) at 90 °C with 1,1- azobis (cyclohexanecarbonitrile) (VAZO-88) as initiator using a (A) linear RAFT agent, (B) a 4-arm star RAFT agent, and (C) a 6-arm-star RAFT agent. Profiles were determined for radical chain lengths of (a) $i = 5$, (b) $i = 10$, (c), $i = 50$, and (d) $i = 100$ in each polymer solution reaction. Also shown (☆) are the conversions at onset of the gel effect, x_{gel}, determined for each chain length.

the rate coefficient for dissociation by translational diffusion, $k_{-\text{trans}}$[69].

$$k_t^{i,i} = \frac{k_{\text{trans}}^{i,i} \times k_{\text{segm}}^{i,i}}{k_{-\text{trans}}^{i,i}} \quad (11)$$

Thus, according to the composite model description of termination (identified above) translational diffusion coefficients such as those obtained using PFG-NMR can only be used to calculate $k_t^{i,i}(x)$ from eq 9 for (i) very short chains in dilute solution, or (ii) radicals in semidilute and concentrated solution conditions when translational diffusion is the rate-determining step. This explains some of the disagreement we noted previously when comparing theoretical models to accurate $k_t^{i,i}$ data obtained for MMA,[12] which gave poor agreement above i_{SL} (=100) in the dilute regime.

From the 3-dimensional $k_t^{i,i}(x)$ vs i vs x data (sees Supporting Information) and eq 9, it is possible to calculate D_i values for polystyrene radical chains in polymerizing solutions up to high conversion for comparison with translational diffusion coefficients reported in the literature. In Figure 8, D_i data is shown for the radical chains $i = 5$, 10, 50, and 100 units, in the region above chain overlap, denoted by a star, where eq 9 can be used. Above the overlap concentration we found that the D_i values were in reasonably good quantitative agreement with diffusion values reported in the literature and showed a very similar dependence on concentration.[17,65,66] This confirms the view that translational diffusion is rate determining in nondilute polymer solutions[70−72] (Figure S8). It is shown here that the RAFT−CLD−T method also provides an indirect means to obtain diffusion coefficients for radical chains of length i in a continually evolving polymer−solvent mixture.

Conclusions

The effect of polymer matrix architecture (polystyrene stars) on the termination of linear polystyrene radical chains has been studied in continually evolving polymer−solvent mixture using the RAFT−CLD−T method. It was found that four distinct regions were observed for the stars analogous to the linear RAFT-mediated polymerizations: (i) termination of short chains in the dilute region, (ii) termination of long chains in the dilute region, (iii) termination above c^* in the semidilute regime, and (iv) termination in the concentrated regime. The dependencies for the 4-arm and 6-arm stars in the dilute regime were similar to that found for the linear polymer (α_S and α_L 0.53 and 0.15, respectively). However, the gel onset conversion (x_{gel}) increased with the greater number of arms on the star, in agreement with the Zimm−Stockmayer prediction and in excellent agreement with the theoretical over lap concentration c^*. This supports our previous work that claimed chain overlap is the main cause of the onset of the gel effect in free-radical polymerizations. The results also showed that the arms were stretched close to the core due to a high polymer segment density, in agreement with literature results. Termination in the concentrated regime showed that the stars had a greater dependence with α_{gel} exponents for both the 4- and 6-arm stars close to $1.82x$ that is much greater than for the linear system ($\alpha_{\text{gel}} = 1.22x$). This result would suggest that reptation controls termination in the concentrated regime, which would predict dependencies of 1.5 or 2. However, the dependencies predicted by reptation will only be reached in our systems at high conversions (close to the glass transition), suggesting that although the constriction points conferred by the star polymers on the matrix there is still a great deal of matrix mobility on the time scale required for diffusion, and that the linear radicals are not confined to a tubelike surrounding, as prescribed by reptation. The RAFT−CLD−T method also provided a means to determine diffusion coefficients for chain length i in the regions where the translational diffusion is rate determining.

Acknowledgment. G.J.-H. acknowledges financial support from the Australian Research Council (ARC), Australian Institute for Nuclear Science and Engineering, and the University of Queensland (UQJRS scholarship). M.J.M acknowledges financial support from the ARC Discovery grant and receipt of a QEII Fellowship (ARC fellowship). We are also very thankful to Dr. Michael Whittaker (UQ) for preparation of the 4-arm star RAFT agent.

Supporting Information Available: A table containing the experimental reaction conditions, figures showing all M_n and PDI data, conversion vs time profiles for all reactions, plots of 3-dimensional $k_t^{i,i}$ vs i vs x profiles for each reaction, and text giving surface fit functions for the 3-dimensional $k_t^{i,i}$ vs i vs x profiles. This material is available free of charge via the Internet at http://pubs.acs.org.

References and Notes

(1) Norrish, R. G. W.; Smith, R. R. *Nature (London)* **1942**, *150*, 336−337.
(2) Ying, Q.; Chu, B. *Macromolecules* **1987**, *20*, 362−366.
(3) Teraoka, I. *Polymer Solutions: An Introduction to Physical Properties*; John Wiley & Sons: New York, 2002.
(4) Johnston-Hall, G.; Monteiro, M. J. *Macromolecules* **2007**, *40*, 7171−7179.
(5) Vana, P.; Davis, T. P.; Barner-Kowollik, C. *Macromol. Rapid Commun.* **2002**, *23*, 952−956.
(6) Johnston-Hall, G.; Theis, A.; Monteiro, M. J.; Davis, T. P.; Stenzel, M. H.; Barner-Kowollik, C. *Macromol. Chem. Phys.* **2005**, *206*, 2047−2053.
(7) Chiefari, J.; Chong, B. Y. K.; Ercole, F.; Krstina, J.; Jeffery, J.; Le, T. P. T.; Mayadunne, R. T. A.; Meijs, G. F.; Moad, C. L.; Moad, G.; Rizzardo, E.; Thang, S. H. *Macromolecules* **1998**, *31*, 5559−5562.
(8) Moad, G.; Rizzardo, E.; Thang, S. H. *Aust. J. Chem.* **2005**, *58*, 379−410.
(9) Adams, M. E.; Russell, G. T.; Casey, B. S.; Napper, D. H.; Gilbert, R. G.; Sangster, D. F. *Macromolecules* **1990**, *23*, 4624.
(10) Russell, G. T.; Napper, D. H.; Gilbert, R. G. *Macromolecules* **1992**, *25*, 2459−2469.
(11) Russell, G. T. *Macromol. Theory. Simul.* **1994**, *3*, 439−468.
(12) Johnston-Hall, G.; Stenzel, M. H.; Davis, T. P.; Barner-Kowollik, C.; Monteiro, M. J. *Macromolecules* **2007**, *40*, 2730−2736.
(13) Tulig, T. J.; Tirrell, M. *Macromolecules* **1981**, *14*, 1501−1511.
(14) De Gennes, P. G. *J. Chem. Phys.* **1982**, *76*, 3322−3326.
(15) Russell, G. T. *Aust. J. Chem.* **2002**, *55*, 399−414.
(16) Gilbert, R. G. *Emulsion Polymerization: A Mechanistic Approach*, 1st ed.; Academic Press: London, 1995; p 362.
(17) Scheren, P. A. C.; Russell, G. T.; Sangster, D. F.; Gilbert, R. G.; German, A. L. *Macromolecules* **1995**, *28*, 3637−3648.
(18) Tirrell, M. *Rubber Chem. Technol.* **1984**, *57*, 523−556.
(19) Graessley, W. W. *Adv. Polym. Sci.* **1982**, *47*, 67−117.
(20) Bauer, B. J.; Fetters, L. J.; Graessley, W. W.; Hadjichristidis, H.; Quack, G. J. *Macromolecules* **1989**, *22*, 2337−2347.
(21) Lodge, T. P.; Markland, P.; Wheeler, L. M. *Macromolecules* **1989**, *22*, 3409−3418.
(22) Grest, G. S. *Macromolecules* **1994**, *27*, 3493−3500.
(23) Colley, R. F.; Collins, S. A.; Richards, R. W. *J. Mater. Chem.* **2003**, *13*, 2765−2770.
(24) Moad, G.; Mayadunne, R. T. A.; Rizzardo, E.; Skidmore, M. A.; Thang, S. H. *Macromol. Symp.* **2003**, *192*, 1−12.
(25) Mayadunne, R. T. A.; Jeffery, J.; Moad, G.; Rizzardo, E. *Macromolecules* **2003**, *36*, 1505−1513.
(26) Mayadunne, R. T. A.; Moad, G.; Rizzardo, E. *Tetrahedron Lett.* **2002**, *43*, 6811−6814.
(27) Bywater, D. J.; Worsford, J. *J. Polym. Sci.* **1962**, *58*, 571.
(28) Pryor, W. A.; Lasswell, L. D. *Advances in Free Radical Chemistry*, 1st ed.; Academic Press: New York, 1975.
(29) Theis, A.; Feldermann, A.; Charton, N.; Davis, T. P.; Stenzel, M. H.; Barner-Kowollik, C. *Polymer* **2005**, *46*, 6797−6809.
(30) Theis, A.; Feldermann, A.; Charton, N.; Stenzel, M. H.; Davis, T. P.; Barner-Kowollik, C. *Macromolecules* **2005**, *38*, 2595−2605.

(31) Feldermann, A.; Stenzel, M. H.; Davis, T. P.; Vana, P.; Barner-Kowollik, C. *Macromolecules* **2004**, *37*, 2404−2410.
(32) Theis, A.; Davis, T. P.; Stenzel, M. H.; Barner-Kowollik, C. *Macromolecules* **2005**, *38*, 10323−10327.
(33) Theis, A.; Davis, T. P.; Stenzel, M. H.; Barner-Kowollik, C. *Polymer* **2006**, *47*, 999−1010.
(34) Johnston-Hall, G.; Monteiro, M. J. Submitted for publication, 2007.
(35) Barner-Kowollik, C.; Vana, P.; Quinn, J. F.; Davis, T. P. *J. Polym. Sci. Part A: Polym. Chem.* **2002**, *40*, 1058−1063.
(36) Monteiro, M. J.; de Brouwer, H. *Macromolecules* **2001**, *34*, 349−352.
(37) Barner-Kowollik, C.; Buback, M.; Charleux, B.; Coote, M. L.; Drache, M.; Fukuda, T.; Goto, A.; Klumpermann, B.; Lowe, A. B.; Mcleary, J. B.; Moad, G.; Monteiro, M. J.; Sanderson, R. D.; Tonge, M. P.; Vana, P. *J. Polym. Sci., Part A: Polym. Chem.* **2006**, *44*, 5809−5831.
(38) Monteiro, M. J. *J. Polym. Sci., Part A: Polym. Chem.* **2005**, *43*, 3189−3204.
(39) Monteiro, M. J. *J. Polym. Sci., Part A: Polym. Chem.* **2005**, *43*, 5643−5651.
(40) van Herk, A. M. *Polym. Rev.* **1997**, *C37*, 633−648.
(41) Cotton, J. P.; Nierlich, M.; Boue, F.; Daoud, M.; Farnoux, B.; Jannink, G.; Duplessix, R.; Picot, C. *J. Chem. Phys.* **1976**, *65*, 1101−1108.
(42) Lodge, T. P.; Muthukumar, M. *J. Phys. Chem.* **1996**, *100*, 13275−13292.
(43) Zimm, B. H.; Stockmayer, W. H. *J. Chem. Phys.* **1949**, *17*, 1301−1314.
(44) Zimm, B. H.; Kilb, R. W. *J. Polym. Sci. Part B: Polym. Phys.* **1996**, *34*, 1367−1390.
(45) North, A.; M;, Reed, G. A. *Trans. Faraday Soc.* **1961**, *57*, 859.
(46) Smith, G. B.; Russell, G. T.; Heuts, J. P. A. *Macromol. Theory. Simul.* **2003**, *12*, 299−314.
(47) Buback, M.; Muller, E.; Russell, G. T. *J. Phys. Chem.* **2006**, *110*, 3222−3230.
(48) Benson, S. W.; North, A.; M. *J. Am. Chem. Soc.* **1962**, *84*, 935−940.
(49) Olaj, O. F.; Zifferer, G. *Makromol. Chem., Rapid Commun.* **1982**, *3*, 549−556.
(50) Friedman, B.; O'Shaughnessy, B. *Macromolecules* **1993**, *26*, 5726−5739.
(51) O'Neil, G. A.; Wisnudel, M. B.; Torkelson, J. M. *Macromolecules* **1996**, *29*, 7477−7490.
(52) Zimm, B. H.; Kilb, R. W. *J. Polym. Sci., Part B: Polym. Phys.* **1959**, *34*, 1367−1390.
(53) Daoud, M.; Cotton, J. P. *J. Phys.* **1982**, *43*, 531.
(54) McLeish, T. C. B. *Europhys. Lett.* **1988**, *6*, 511−516.
(55) Fetters, L. J.; Lohse, D. J.; Colby, R. H.; Chain Dimensions and Entanglement Spacings. In *Physical Properties of Polymers Handbook*, Mark, J. E., Ed.; Springer: Berlin, 2006; p 445.
(56) Turner, D. T. *Macromolecules* **1977**, *10*, 221−225.
(57) Lee, H. B.; Turner, D. T. *Macromolecules* **1977**, *10*, 231−235.
(58) Lee, H. B.; Turner, D. T. *Macromolecules* **1977**, *10*, 226−231.
(59) High, K. A.; Lee, H. B.; Turner, D. T. *Macromolecules* **1979**, *12*, 332−337.
(60) Roovers, J.; Hadjichristidis, H.; Fetters, L. J. *Macromolecules* **1983**, *16*, 214−220.
(61) Lantman, C. W.; MacKnight, W. J.; Rennie, A. R.; Tassin, J. F.; Monnerie, L. *Macromolecules* **1990**, *23*, 836−838.
(62) Hutchings, L. R.; Richards, R. W.; Reynolds, S. W.; Thompson, R. L. *Macromolecules* **2001**, *34*, 5571−5578.
(63) Griffiths, M. C.; Strauch, J.; Monteiro, M. J.; Gilbert, R. G. *Macromolecules* **1998**, *31*, 7835−7844.
(64) Hanley, B.; Tirrell, M.; Lodge, T. P. *Polym. Bull. (Berlin)* **1985**, *14*, 137−142.
(65) Piton, M. C.; Gilbert, R. G.; Chapman, B. E.; Kuchel, P. W. *Macromolecules* **1993**, *26*, 4472−4477.
(66) Chekal, B. P.; Torkelson, J. M. *Macromolecules* **2002**, *35*, 8126−8138.
(67) von Smoluchowski, M. *Phys. Chem.* **1917**, *92*, 129.
(68) Benson, S. W.; North, A.; M. *J. Am. Chem. Soc.* **1959**, *81*, 1339−1345.
(69) Odian, G. *Principles of Polymerization.* New York: Wiley-Interscience: 1991.
(70) Cardenas, J. N.; O'Driscoll, K. *J. Polym. Sci., Part A: Polym. Chem.* **1977**, *15*, 2097−2018.
(71) Mahabadi, H. K.; O'Driscoll, K. *J. Polym. Sci.: Polym. Chem. Ed.* **1977**, *15*, 283−300.
(72) Dionisio, J.; Mahabadi, H. K.; O'Driscoll, K.; Abuin, E.; Lissi, E. A. *J. Polym. Sci., Part A: Polym. Chem.* **1979**, *17*, 1891−1900.
(73) Buback, M.; Gilbert, R. G.; Hutchinson, R. A.; Klumpermann, B.; Kutcha, F.-D.; Manders, B. G.; O'Driscoll, K.; Russell, G. T.; Schweer, J. *Macromol. Chem. Phys.* **1995**, *196*, 3267−3280.
(74) Brandup, J.; Immergut, E. H.; Grulke, E. A. *Polymer Handbook*, 4th ed.; J. Wiley & Sons: New York, 1999.
(75) Bovey, F. A. *Chain Structure and Conformation of Macromolecules*; Academic Press: New York, 1982.

MA702569M